Anal. Bioanal. Electrochem., Vol. 8, No. 5, 2016, 604-614

Analytical & Bioanalytical Electrochemistry

2016 by CEE
www.abechem.com

Full Paper

Preparation and Characterization of Poly(Vinyl pyrrolidone)/Polyvinyl Chloride Coated Superparamagnetic Iron Oxide (Fe_3O_4) Nanoparticles for Biomedical Applications

Isa Karimzadeh,[1] Mustafa Aghazadeh[2,*] and Taher Doroudi[1]

[1]*Shefa Neuroscience Research Center, Khatam ol Anbia Specialty and Subspecialty Hospital, Tehran, Iran*

[2]*NFCRI, Nuclear Science and Technology Research Institute (NSTRI), P.O. Box 14395-834, Tehran, Iran*

*Corresponding Author, Tel.: +982182064289; Fax: +982182064289

E-Mail: maghazadeh@aeoi.org.ir

Received: 27 July 2016 / Accepted: 31 July 2016 / Published online: 15 August 2016

Abstract- Superparamagnetic Fe_3O_4 nanoparticles double coated with poly(vinylpyrrolidone)/polyvinyl chloride polymers were successfully fabricated by a facile cathodic electrochemical deposition (CED) method. In this method, *in situ* polymer coating ofthe surface of Fe_3O_4 nanoparticles was achieved through electrodeposition process. The evaluation by XRD analysis confirmed that the electrodeposited nanoparticles are composed of pure phase of iron oxide i.e. magnetite (Fe_3O_4). The structure and composition of the prepared nanoparticles were characterized by SEM, TEM, DLS, XRD, FTIR, and TG analysis. The DLS analysis revealed that the bare and prepared polymer coated Fe_3O_4 nanoparticles have size of 20nm and 62nm, respectively. The polymer coated nanoparticles with having 15nm in size, suitable magnetization value (*Ms*=22 emu/g), and negligible coercivity (*Ce*=0.42 emu/g) and remanence (*Mr*=1.1 Oe) are proper candidate for biomedical applications. This electrochemical strategy is proposed as facile and efficient for preparation and double coating of Fe_3O_4 nanoparticles.

Keywords- Nanoparticles, Cathodic electrochemical deposition, Polymer coating, Biomedical Applications

1. INTRODUCTION

In the recent decade, there has been a considerable development of magnetite nanoparticles (MNPs) for biomedical applications like magnetic carriers for drug delivery and targeting supported by external magnetic fields, magnetic resonance imaging (MRI) contrast agents for clinical diagnosis, cancer therapy compounds for hyperthermia, etc. [1-3]. The magnetite (Fe_3O_4)NPs represent superparamagnetic behavior as a result of the infinitely small coercivity arising from the negligible energy barrier in the hysteresis of the hysteresis loop of the particles as predicted by Bloch and Neel [5]. Magnetic nanoparticles for biomedical applications are usually constructed by a Fe_3O_4core, and a biocompatible coating layer such as polymer, amino acid, peptide and polysaccharide [4-6]. The polymeric coating of magnetic nanoparticles is important to improve its stability by decreasing or preventing agglomeration of the nanoparticles. Fe_3O_4 is the most commonly candidate for biomedical applications because of the lower toxicity and suitable magnetic properties. The physicochemical properties of Fe_3O_4 nanoparticles such as their size, shape, hydrophilic nature, coating and surface charge play key role in biodistribution and biocompatibility [7]. Hence, it has been goal of many studies to find a novel and efficient route for preparation of magnetite NPs, and/or modify the common preparation methods, which result Fe_3O_4 nanoparticles with better physicochemical properties, and it is also possible to surface coating during the synthesis procedure. The *in situ* surface coating of magnetite NPs during preparation procedure prevents their agglomeration and increases the magnetic performance. The aggregated form of Fe_3O_4 nanoparticles prevents them to exhibit single particle behavior and the advantages of the nanometer size [4].

Up to now, different chemical-base preparation routes have been used forsynthesize Fe_3O_4nanoparticles, such asco-precipitation, sol-gel, microemulsion, solvothermal, hydrothermal and high temperature decomposition of organic precursors [8-14]. These methods may be able to prepare magnetite with several controllable particle diameters. However, well-dispersed aqueous Fe_3O_4 nanoparticles have met with very limited success.

As one convenient and cheap method, cathodic electrochemical deposition (CED) method has the potential to meet the increasing demand for the direct preparation of well-dispersed Fe_3O_4 nanoparticles and offer a low-temperature alternative to conventional powder synthesis techniques in the production of nanoparticles, and the size distribution of nanoparticles can be well-controlled by manipulating the current and voltage of deposition [15,16]. It was reported that CED route can produce fine, high-purity, fine particles of single and metal oxides and hydroxides [17-23].However, CED procedure has been rarely applied for the preparation of Fe_3O_4 nanoparticles [24-27]. Furthermore, very recently, we reported that in situ surface coating of Fe_3O_4 nanoparticles with biocompatible polymers can be successfully performed during the deposition process [15,16].

In current study, we applied the cathodic electrodeposition for one-pot and *in situ* preparation of polymer coated MNPs with desired size and dispersion from aqueous electrolyte. The poly(vinylpyrrolidone) (PVP) and polyvinyl chloride (PVC) were used as coatings for MNPs during the CED procedure. Notably, this one-step electrochemical preparation of double coated MNPs has not been reported until now. The purity, well-dispersion, nanosize and superparamagnetic property of the prepared MNPs were confirmed via XRD, SEM, VSM and IR techniques. The polymer coat of MNPs was also confirmed via FT-IR, TG and DLS analyses. In spite of the most used chemical routes which require long time (8-12 h) and high temperature (60-80 °C) for coating process, our developed method is *in situ*, simple, one-pot and time conserving.

2. MATERIALS AND METHODS

2.1. Materials

All chemicals used in the synthesis process were reagent grade and were used without further purification. ferricchloride hexahydrate $FeCl_3$.$6H_2O$ (99%), ferrouschloride tetrahydrate $FeCl_2.4H_2O$ (>99%) were obtained from Merck company, Germany. Polyvinylpyrrolidone (PVP, Mw~1,300,000, by LS) and poly vinyl chloride (PVC, Mw~48000) were purchased from Sigma-Aldrich. Deionized water was used in all experiments.

2.2. Preparation of iron oxide nanoparticles

Bare iron oxide was prepared by cathodic electrochemical deposition (CED) procedure. A solution of 0.005 M [$FeCl_3/FeCl_2$] with molar ratio of 2:1 was prepared and used as the electrolyte. The electrochemical set-up included a cathodic stainless-steel cathode centered between two graphite anodes. Electrosynthesis process was performed in the direct current (DC) mode. Prior to each deposition, the steel substrates were galvanostatically electropolished at a current density of 0.5 A cm^{-2} for 5 min in a bath (70^oC) containing 50 vol% phosphoric acid, 25 vol% sulfuric acid and balanced deionized water [18].The deposition experiments were performed using an electrochemical workstation system (Potentiostat/Galvanostat, Model: NCF-PGS 2012, Iran).The current density and deposition time were 10 $mA/cm^2$and 30 min, respectively. After the deposition, the black deposit formed on the steel cathode were scraped and rinsed several times with water. Then the obtained black powder dried at 50 °C for 1h, and used for characterization step.

2.3. Preparation of polymer coated iron oxide nanoparticles

The same electrochemical set-up including stainless-steel and graphite electrode was also used for preparation of coated nanoparticles. In this way, a solution of 0.005 M [$FeCl_2/FeCl_3$]

with molar ratio of 1:2 was prepared, and coating agents including 1 gr/L PVP and 1 gr/L PVC] were then added into the prepared solution. The obtained mixture was used as deposition electrolyte. The electrosynthesis process was done from this electrolyte solution by applying DC mode of 10 $mAcm^{-2}$ for 1 hr. After the deposition, the steel cathode was rinsed with distilled water several times and the black deposit formed onto its surface was scraped. The obtained deposit was dissolved and washed several times with ethanol for removal of free PVP and PVC. In final, the black deposit was separated from ethanol solution with magnet, and dried at 50 °C for 1h. The powder was evaluated by further analyses.

2.4. Instrumentation

The morphology of the deposited nanoparticles was observed by field-emission scanning electron microscope (FE-SEM, TE-SCAN Model MIRA3, operating voltage 30 kV) and transmission electron microscope (TEM, Zeiss EM 900). Nanoparticle powder for TEM measurements were suspended in ethanol and supported on a carbon-coated copper grid. The crystal structure of obtained black powders was determined by powder X-ray diffraction (XRD, a Phillips PW-1800 diffractometer with Co Kα radiation (λ=1.789 Å)). Fourier transform infrared (FT-IR) spectra were obtained on a Nicolet AVATAR 330FT-IR spectrophotometer using KBr pressing method. The FTIR spectrum was recorded using transmissive mode and the spectrum was collected at room temperature in the 4000–400 cm^{-1}range with a resolution of 4 cm^{-1}using 20 scans. Thermogravimetric analysis (TGA) was conducted with a simultaneous TG/DSC STA1500 thermal analysis system (Netzsch) between room temperature and 600^{o}C, at a heat in grate of 10^{o}C min^{-1} in nitrogen atmosphere. The magnetic properties were measured at room temperature using a Lake shore vibrating sample magnetometer (VSMModel-7400).The hysteresis loops was recorded from −20000 to 20000 Oe. The mean particle sizes were determined using a dynamic light scattering (DLS) technique (Malvern Instruments).

3. RESULT AND DISCUSSION

Fig. 1 shows that the XRD patterns of the prepared NPs. It is clearly acceptable the crystalline nature and magnetite phase of the prepared material and based on the comparison of their XRD patterns with the standard pattern of Fe_3O_4 (JCPDS 75-0033). The diffraction peaks corresponding to (220), (311), (400), (511) and (440) are quite identical to the characteristic peaks of the Fe_3O_4crystal structure. No peak related to the any impurity was observed. The crystallite size has been estimated from the XRD pattern using the Scherrer's equation ($D=0.9\lambda/\beta \cos(\theta)$), where, β is the full width at half maxima (FWHM) of the (311) peak. The average crystallite size of uncoated and coated Fe_3O_4-NPs was calculated to be 10.2 nm and8.7 nm, respectively.

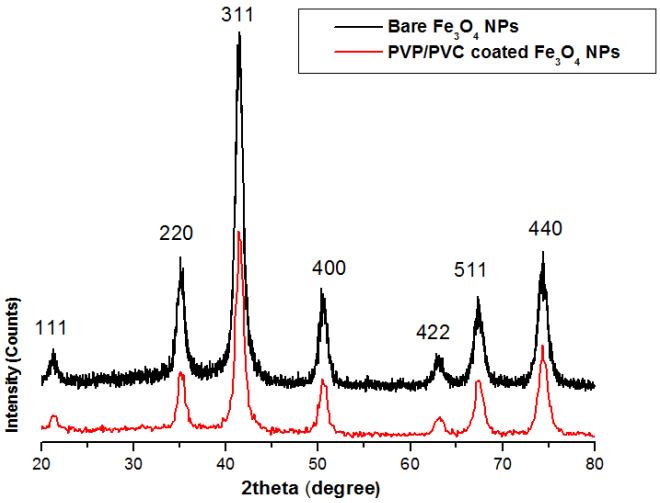

Fig. 1. XRD patterns of the prepared (a) bare and (b) PVP/PVC coated Fe_3O_4 nanoparticles

The PVP/PVC coat on the surface of deposited nanoparticles was confirmed by FTIR spectroscopy. Fig. 2 shows the IR spectra of the prepared nanoparticles. For bare nanoparticles, the band at 556 cm^{-1} is related to the stretching mode of Fe-O in Fe_3O_4 [15,16], indicating the magnetite phase of the prepared sample. The absorption bands at 3465 and 1632 cm^{-1} are related to O–H stretching and deformation vibrations, respectively. These bands indicated the existence of hydroxyl groups connected to the surface of Fe_3O_4 nanoparticles [24].

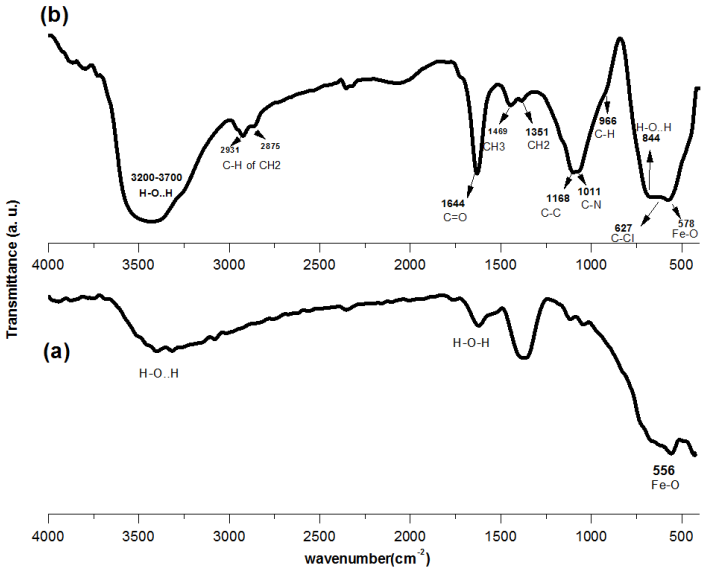

Fig. 2. FT-IR spectra of the prepared (a) bare and (b) PVP/PVC coated Fe_3O_4 nanoparticles

In the spectrum of coated nanoparticles, there are some new IR bonds, which can be assigned to the existence of PVP and PVC polymers. In fact, the following bands confirmed the PVP and PVC polymers are coated on the surface of Fe_3O_4 NPs during the CED synthesis: (i) the bonds at 1168 cm^{-1} and 1332 cm^{-1} are due to the stretch and vibration of C-C bands (antisymmetric stretch), respectively [28,29], (ii) the peaks at about 1351 cm^{-1} and 1469 cm^{-1} are assigned to the CH_2 vibrations [30], (iii) the peaks at 2931 cm^{-1} and 2875 cm^{-1} deal with to the asymmetric and symmetric stretching vibrations of C-H bonds, respectively [31], (iv) the bonds around 966 cm^{-1} indicating the bending vibrations of CH out-of-plane [32,33], (v) the peaks at 1011 cm^{-1} deal with to the C-N stretching mode and is characteristic peak of PVP, where revealing the presence of PVP coat on the surface nanoparticles, and (vi) the peak at 627 cm^{-1} is also related to the stretching vibration of C-Cl bond in PVC [33]. Furthermore, C=O group vibrations are observed at 1644 cm^{-1}. Notably, the C=O vibration is seen at about 1660-1670 cm^{-1} for pure PVP [30,34]. The C=O band shifted from 1670 to 1644 cm^{-1} indicates the chemical interaction between C=O groups and the Fe_3O_4 nanoparticles. Finally, it can be clearly seen that the IR spectra of the coated nanoparticles have all the characteristic vibrations peaks of PVP and PVC including CH_2 and CH_3 groups, C=O, C-C, C-Cl, and C-N bonds. These results completely confirmed the presence of PVP/PVC layer on the surface of the electrodeposited NPs.

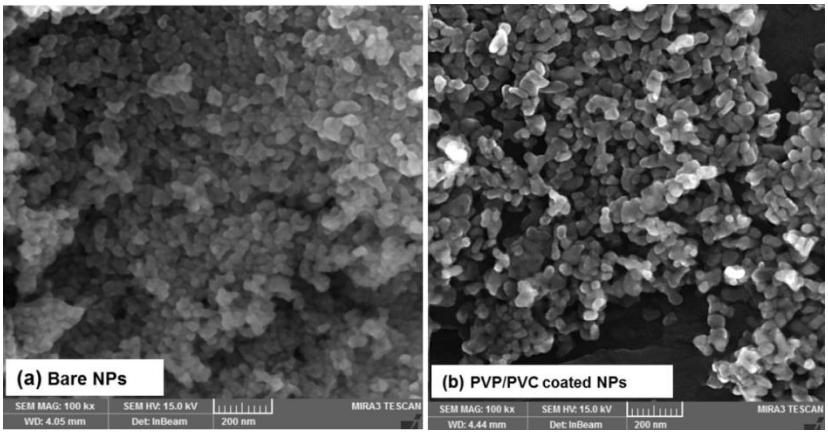

Fig. 3. FE-SEM images of the prepared (a) bare and (b) PVP/PVC coated Fe_3O_4 nanoparticles

Fig. 3 shows the morphological observations obtained by FE-SEM technique. It is clearly seen that both uncoated and coated samples have particle morphology at nanoscale. The uncoated or bare Fe_3O_4 has a little agglomerated particles with their size are in range of 15-20 nm. The coated sample exhibits less agglomerated and its nanoparticles have mean diameter of 20 nm (Fig. 3b).

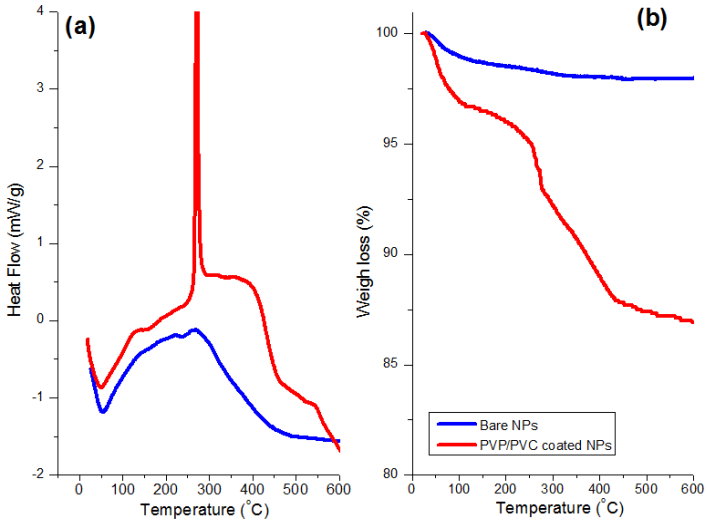

Fig. 4. DSC-TG curves for the prepared (a) bare and (b) PVP/PVC coated Fe_3O_4 nanoparticles

The thermal stability and weight loss change of the prepared nanoparticles on heating was studied thermogravimetric analysis. Fig. 4 shows DSC and related TG curves for both uncoated and coated nanoparticles. For our samples, a multistep exothermic peak is observed in DSC curve between the temperatures of 100 and 600°C. Correspondingly, TG curve shows three major weight losses at these temperatures. At temperatures below 100°C, the observed weight losses is related to removal of the H_2O molecules connected on the surface of SPIONs as confirmed by FT-IR analysis. In the literature, it was reported that PVC degradation is occurred at 200-250°C [36-40].

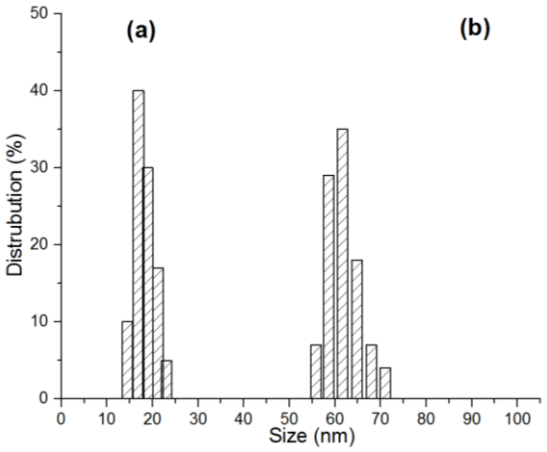

Fig. 5. Particle size distributions of (a) bare and (b) PVP/PVC coated Fe_3O_4 nanoparticles

Hence, the sharp change in DSC and TG curved at 225-250°C is due to the PVC decomposition. The mass loss during PVC degradation includes sequential loss of hydrogen

chloride accompanied by the generation of polyene sequences [36-38]. It was also reported that pure PVP is started to decompose at about 380°C, whereas for PVP coated on Pt nanoparticles, the decomposition happens at 350°C, 30°C lower than that for pure PVP [39]. So, the weight loss observed at the temperature range of 300-400°C is mainly related to PVP decomposition from the NPs surface. The TG curve exhibit the total weight losses of 12.6%, which confirmed the presence of PVP/PVC coat onto the surface of the deposited nanoparticles. These results confirmed the *in situ* double coating of the Fe_3O_4 nanoparticles during their CED procedure.

The hydrodynamic diameter of the bare and polymer coated nanoparticles was measured by a DLS particle size analyzer. Fig. 5 shows the particle size distributions of the bare and polymer coated nanoparticles. For bare NPs (Fig. 5a), the mean hydrodynamic diameter was measured to be about 20 nm. For the polymer coated NPs, this values is observed to be 62 nm, which are larger than those of bare NPs. These results clearly prove the polymer layer on the surface of magnetite nanoparticles.

The magnetization performance of the prepared Fe_3O_4 nanoparticles were valuated at room temperature using vibrating sample magnetometer (VSM), as shown in Fig. 6. It can be seen that the magnetization curve has s-shaped over the applied magnetic field and the samples exhibit typical superparamagnetic behavior, showing high saturation magnetization (M_s)value and negligible coercivity *(Ce)* and magnetic remanence (M_r)values. For bare sample these values are M_s=72 emu/g, M_r=0.71 emu/g and *Ce* =2.3 Oe. For PVP/PVC coated nanoparticles, M_s=22 emu/g, M_r=0.3 emu/g and *Ce* =1.95 Oe were calculated from the M-H curves. These values are completely proved the prepared polymer coated nanoparticles have proper characteristics for biomedical applications.

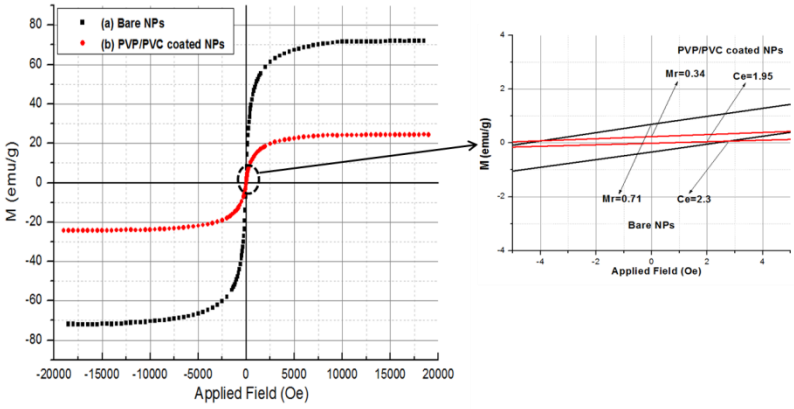

Fig. 6. VSM curves for the prepared (a) bare and (b) PVP/PVC coated Fe_3O_4 nanoparticles

4. CONCLUSION

In final, an innovative and efficient method was established for preparation of double coated Fe_3O_4 nanoparticles. The prepared bare and PVP/PVC coated nanoparticles have

crystal structure of magnetite with size of 10 and 15nm, respectively, as confirmed by XRD and FE-SEM. Optimum electrochemical conditions for preparation of these nanoparticles was found to be applied current density of 10 mA/cm^2, deposition time of 30min and bath composition of0.005 M [$FeCl_2/FeCl_3$] with molar ratio of 1:2.FI-IR and DTA-TG analyses confirmed the polymer layer on the surface of electrodeposited nanoparticles. The results confirmed the proper size and distribution, polymer coat and magnetic properties of the prepared Fe_3O_4 nanoparticles for biomedical applications.

REFERENCES

[1] K. Ulbrich, K. Hola, V. Subr, A. Bakandritsos, J. Tucek, and R. Zboril, Chem. Rev. 116 (2016) 5338.

[2] J. Shan, L. Wang, H. Yu, J. Jia, W. A. Amera, Y. Chena, G. Jinga, H. Khalida, M. Akrama, and N. M. Abbasia. Mater. Sci. Technol. 32 (2016) 602.

[3] M. Calero, L. Gutierrez, G. Salas, Y. Luengo, A. Lazaro, P. Acedo, M. P. Morales, R. Miranda, and A. Villanueva, Nanomed.: Nanotech. Bio. Med. 10 (2014) 733.

[4] M. Wabler, W. Zhu, M. Hedayati, A. Attaluri, H. Zhou, J. Mihalic, A. Geyh, T. L. DeWeese, R. Lvkov, and D. Artemov, Int. J. Hyperthermia. 30 (2014)192.

[5] P. Majewski, and Thierry B, Critical Rev. Solid State Mater. Sci. 32 (2007) 203.

[6] Y. Wang, B. Li, F. Xu, D. Jia, Y. Feng, and Y. Zhou, J. Biomater. Sci. Polym. Ed. 23 (2012) 843.

[7] D. Ling, N. Lee, and T. Hyeon, Acc. Chem. Res. 48 (2015) 1276.

[8] T. T. Dung, T. M. Danh, and L. T. M. Hoa, J. Exp. Nanosci. 4 (2009) 259.

[9] R. Hufschmid, H. Arami, R. Matthew Ferguson, M. Gonzales, E. Teeman, L. N. Brush, N. D. Browning, and K. M. Krishnan, Nanoscale 7 (2015) 11142.

[10] O. M. Lemine, K. Omri, B. Zhang, L. El Mir, M. Sajieddine, A. Alyamani, and M. Bououdina, Superlatt. Microstruct. 52 (2012) 793.

[11] X. D. Liu, H. Chen, S. S. Liu, L. Q. Ye, and Y. P. Li, Mater. Res. Bull. 62 (2015) 217.

[12] S. Li, T. Zhang, R. Tang, H. Qiu, C. Wang, and Z. Zhou, J. Magn. Magn. Mater. 379 (2015) 226.

[13] Z. Wang, J. Zhu, Y. Chen, K. Geng, N. Qian, L. Cheng, Z. Lu, Y. Pan, L. Guo, Y. Li, and H. Gu, RSC Adv. 4 (2014) 7483.

[14] K. Mandel, M. Straber, T. Granath, S. Dembski, and G. Sextla, Chem. Commun. 51 (2015) 2863.

[15] I. Karimzadeh, H. Rezagholipour Dizaji, and M. Aghazadeh, J. Magn. Magn. Mater. 416 (2016) 81.

[16] I. Karimzadeh, M. Aghazadeh, M. R. Ganjali, P. Norouzi, S. Shirvani-Arani, T. Doroudi, P. H. Kolivand, S. A. Marashi, and D. Gharailou, Mater. Lett. 179 (2016) 5.

[17] M.Aghazadeh, T. Yousefi, and M. Ghaemi, J. Rare Earths 30 (2012) 236.

[18] M. Aghazadeh, M. Asadi, M. Ghannadi Maragheh, M. R. Ganjali, P. Norouzi, and F. Faridbod, Appl. Surf. Sci. 364 (2016)726.
[19] R. Cheraghali, and M. Aghazadeh, Anal. Bioanal. Electrochem. 8 (2016) 64.
[20] M. Aghazadeh, A. A. M. Barmi, and M. Hosseinifard, Mater. Lett. 73 (2012) 28.
[21] M. Aghazadeh, A. A. M. Barmi, D. Gharailou, M. H. Peyrovi, and B. Sabour, Appl. Surf. Sci. 283 (2013) 871.
[22] M. Aghazadeh, M. Ghannadi Maragheh, M. R. Ganjali, P. Norouzi, and F. Faridbod, Appl. Surf. Sci. 364 (2016) 141.
[23] M. Aghazadeh, M. R. Ganjali, and P. Norouzi, Mater. Res. Express 3 (2016) 055013.
[24] R. F. C. Marques, C. Garcia, P. Lecante, S. J. L. Ribeiro, L. Noe, N. J. O. Silva, V. S. Amaral, A. Millan, and M. Verelst, J. Magn. Magn. Mater. 320 (2008) 2311.
[25] M. Ibrahim, K. G. Serrano, L. Noea, C. Garcia, and M. Verelst, Electrochim. Acta 55 (2009) 155.
[26] H. Park, P. Ayala, M. A. Deshusses, A. Mulchandani, H. Choi, and N. V. Myung, Chem. Engin. J. 139 (2008) 208.
[27] N. Salamun, H. Xin Ni, S. Triwahyono, A. Abdul Jalil, and A. Hakimah Karim, J. Fundamental Sci. 7 (2011) 89.
[28] Y. Junejo, A. Baykal, and H. Sozeri, Cent. Eur. J. Chem. 11 (2013) 1527.
[29] Z. J. Zhang, X. Y. Chen, B. N. Wang, and C. W. Shi, J. Crys. Growth 310 (2008) 5453.
[30] Y. Zhang, J. Y. Liu, S. M. Jing, X. Zhao, X. D. Zhang, and Z. D. Zhang, J. Mater. Sci: Mater. Med. 21 (2010) 1205.
[31] Z. Tu, B. Zhang, G. Yang, M. Wang, F. Zhao, D. Sheng, and J. Wang, Colloids Surf. A 436 (2013) 854.
[32] S. Mohapatra, N. Pramanik, S. K. Ghosh, and P. Pramanik, J. Nanosci. Nanotech. 6 (2006) 823.
[33] C. Barrera, A. P. Herrera, N. Bezares, E. Fachini, R. Olayo-Valles, J. P. Hinestroza, and C. Rinaldi, J. Colloid Interf. Sci. 377 (2012) 40.
[34] H. Y. Lee, N. H. Lim, J. A. Seo, S. H. Yuk, B. K. Kwak, G. Khang, H. B. Lee, S. H. Cho, J. Biomed. Mater. Res. B 102 (2008) 1.
[35] A. Masoudi, H. R. Madaah Hosseini, M. A. Shokrgozar, R. Ahmadi and M. A. Oghabian, Int. J. Pharmaceut. 433 (2012) 129.
[36] M. Kok, K Demrelli, and Y. Aydogdu, Int. J. Sci. Technol. 3 (2008) 37.
[37] B. Li, Polymer Degradation and Stability 68 (2000) 197.
[38] S. Santra, R. Tapec, N. Theodoropoulou, J. Dobson, A. Hebard, and W. Tan, Langmuir 17 (2001) 2900.
[39] Y. K. Du, P. Yang, Z. G. Mou, N. P. Hua, and L. Jiang, J. Appl. Polymer Sci. 99 (2006) 23.

[40] K. Yao, J. Gong, N. Tian, Y. Lin, X. Wen, Z. Jiang, H. Na, and T. Tang, RSC Adv. 5 (2015) 31910.

Copyright © 2016 by CEE (Center of Excellence in Electrochemistry)

ANALYTICAL & BIOANALYTICAL ELECTROCHEMISTRY (http://www.abechem.com**)**

Reproduction is permitted for noncommercial purposes.